PHOTOCATALYTIC HYDROGEN EVOLUTION ACTIVITY OF ANATASE-BROOKITE NANOPARTICLES MODIFIED WITH RARE EARTH METALS (Gd, Lu, Tm, Tb, Pr)

[1, 2]Tetiana KHALIAVKA, [3]Nataliya SHCHERBAN, [3]Ganna KORZHAK, [3]Pavel YAREMOV, [3]Ivan KOPA, [1]Regina BURVE, [1]Elif COŞKUN, [1]Jean-Claude GRIVEL

[1]Technical University of Denmark, Department of Energy Conversion and Storage, Lyngby, Denmark, EU, tekha@dtu.dk

[2]Institute for Sorption and Problems of Endoecology NASU, Kyiv, Ukraine, EU

[3]L.V. Pisarzhevskii Institute of Physical Chemistry NASU, Kyiv, Ukraine, EU

https://doi.org/10.37904/nanocon.2025.4988

Abstract

Rare earth elements (Gd, Lu, Tm, Tb, Pr) modification effects on two-phased TiO_2 (anatase-brookite) were analyzed. The powders were synthesized by a one-step hydrothermal method. The phase composition, crystalline size, and shape of the samples were studied by X-ray diffractometry, transmission and scanning electron microscopies, and energy-dispersive X-ray spectroscopy. The decrease of the crystallite size and increase of the lattice strain due to the modification were confirmed by the Scherrer, modified Scherrer, Williamson-Hall, Size-strain plot (SSP), and Halder-Wagner methods. The textural characteristics of the samples were determined from N_2 adsorption-desorption isotherms using the methods of Brunauer–Emmet–Teller and Barret–Joiner–Halenda and revealed their mesoporous structure. UV-Vis diffuse reflectance spectra of the modified samples showed a blue shift compared to the unmodified sample. The values of band gap energy of the modified powders increased due to a phenomenon of quantum confinement or size quantization. The modification with rare earth elements improved the photocatalytic activity of the anatase-brookite composite in the hydrogen evolution reaction, which was ascribed to physico-chemical properties.

Keywords: Rare earth elements, anatase-brookite nanoparticles, photocatalysis, hydrogen

1. INTRODUCTION

Titanium dioxide (TiO_2) is the most widely used photocatalyst, which exists in three main forms: anatase, rutile and brookite. Anatase is considered the most active form, but it has some disadvantages, such as a wide band gap, a high recombination rate of the photogenerated electron-hole pairs, etc.

To improve the photocatalytic properties of TiO_2, researchers have tried two- or three-phased compositions based on anatase, rutile, or brookite as photocatalysts. It was established that two-phased TiO_2 (P25 Degussa), which contains anatase and rutile, shows high activity because it can effectively stimulate electron transfer from one phase to another thereby improving photocatalytic properties [1].

Recent reports have indicated that anatase-brookite composites demonstrate better photocatalytic performance due to the synergistic effect between these two phases [2]. Also, during the photocatalytic reaction electrons transfer from the more cathodic conduction band of brookite to the anatase conduction band favouring an effective electron–hole separation [3]. Besides, brookite has an appropriate electron trap depth for prolongation of the lifetime of photogenerated electrons and holes and special connection of the octahedral chain leads to exposed O atoms, which can be used as catalytic active atoms and enhance the catalytic activity [1]. Therefore, two-phased TiO_2 containing brookite is a promising material for photocatalysis.

Another way to improve photocatalytic activity is modification, where rare earth elements deserve special attention as dopants. Using these dopants allows to tune structural, optical, textural, morphological, etc. characteristics of TiO_2 [4-10]. Rare earth elements as modifiers for TiO_2 can create defects and oxygen vacancies [11], tuning the bandgap, extending the adsorption spectrum into the visible region, and enhancing the charge separation and transfer processes that favour photocatalytic processes [4-10]. Such materials can be active in the reaction of photocatalytic hydrogen (H_2) evolution. It is known that hydrogen has been suggested as an alternative fuel because it can be eco-friendly and clean depending on its production method. The use of hydrogen allows to avoid greenhouse gas emissions.

In this study the influence of modification of two-phased anatase-brookite TiO_2 (*AB*) with rare earth elements (*RE*) (Gd, Lu, Tm, Tb, Pr) on structural, optical, textural, and photocatalytic properties was analysed. The photocatalytic activity was evaluated in the reaction of hydrogen evolution from water-ethanol solutions under UV light.

2. EXPERIMENTAL

2.1 Samples synthesis

The unmodified and modified with *RE* (Gd, Lu, Tm, Tb, Pr) *AB* nanopowders were synthesized by a one-step hydrothermal method. In a typical synthesis, 40 ml of distilled water or 40 ml solution of rare earth metal acetate (Alfa Aesar) (~2% molar amount per titanium atoms) were applied for the synthesis of *AB* and *RE/AB*, respectively. Then titanium butoxide ($Ti(OBu)_4$) (Aldrich) was slowly added to this solution under continuous stirring. Afterward, the solution was transferred into a Teflon-lined autoclave with a capacity of 100 ml for 24 h at 150°C. The heating rate was 5°C/min. Synthesis was carried out at an initial pH of 10.5. After the cooling of the autoclave to room temperature, the samples were washed with distilled water and dried in the oven at 60 °C for 24 h.

2.2 Characterization

The phase composition of the samples was determined by X-ray diffraction (XRD) method using an Aeris diffractometer (PANalytical) with Cu Kα radiation (λ = 1.5418 Å). The crystallite size was evaluated by the Scherrer (D_{Sch} and $D_{Sch(Aver)}$) and modified Scherrer equation (D_{MSch}), the Williamson-Hall method based on uniform deformation model ($D_{W\text{-}H\text{-}UDM}$), uniform stress deformation model ($D_{W\text{-}H\text{-}USDM}$), and Uniform deformation energy density model ($D_{W\text{-}H\text{-}UDEDM}$) approaches, Size-strain plot (D_{SSP}) and the Halder-Wagner method ($D_{H\text{-}W}$).

Raman spectra of the prepared samples were recorded using an InVia Raman Spectrometer (Renishaw), UK with laser emitting at the excitation wavelengths of 532 nm (100 mW max. power output. To record the spectrum, the laser was set to 10 mW power, total excitation time was 15 seconds (3s x 5).

The morphology, crystallites size and element composition of the samples were studied by scanning electron microscopy (SEM) using a Zeiss Merlin FEGSEM microscope, and a Tabletop TM3000 Hitachi SEM microscope with EDS as well a transmission electron microscopy (TEM) using a Tecnai T20 G2 microscope with a 200 kV accelerating voltage (DTU National Centre for Nano Fabrication and Characterization).

The room-temperature FT-IR spectra of the samples were recorded using a Bruker Tensor 27 FT-IR Spectrometer. UV-Vis diffuse reflectance spectra (DRS) of the powders were measured using a Perkin-Elmer Lambda Bio 35 spectrophotometer. The band gap values (E_g) was estimated using the Wood and Tauc method.

The porous structure of the samples was studied by nitrogen adsorption using a Micromeritics 3Flex instrument. Textural characteristics were determined from N_2 adsorption–desorption isotherms using the methods of Brunauer–Emmet–Teller (BET) and Barret–Joiner–Halenda (BJH).

2.3 Photocatalytic experiments

In a typical experiment of photocatalytic hydrogen evolution, a sample of photocatalyst (0.03 g) was dispersed in 10.0 ml of aqueous solution containing 2 mol/l ethanol (electron donor) in cylindrical glass thermostatic reactors. Co-catalyst Pd/SiO_2 (0.01 g,) was obtained employing $PdCl_2$ reduction with hydrogen on the surface of commercial silica in an alcohol solution (1 wt. % palladium on SiO_2) and was added into the mixture. The reaction mixture was degassed before irradiation using a vacuum pump. The suspension was stirred and irradiated with a high-pressure mercury lamp (DRSH 1000; 1000 W; λ_{max} = 365nm; 50 mW/cm^2), T = 40 ^{0}C. The composition of the gas phase above the solution was determined every 30 min chromatographically. The experiment with each sample was repeated three times.

3. RESULTS AND DISCUSSIONS

The synthesized powders consist of agglomerates containing roundly elongated crystallites (**Figure 1a**). **Figure 1b** shows XRD patterns for *AB* and *RE/AB*. The diffraction peaks at the 2θ ~ 25.3°, 37.8°, 48.0°, 54.0°, 62.7°, 75.1° were indexed to anatase phase according to standard JCPDS Card no. 96-900-9087 and assigned to (101), (004), (200, (105), (204), (215) planes, respectively. The samples' unit cell parameters, unit cell volumes, and axial ratios indicated the tetragonal crystal structure of the samples which is characteristic for anatase. Besides these peaks, the peak at 2θ ~ 30.8° was fixed and related to the (121) crystal plane of brookite according to JCPDS Card no. 96-900-4141. No characteristic peaks were detected for rutile phase.

The Raman spectra (**Figure 1c**) of the samples also showed anatase bands at 144, 199, 399, 517 and 639 cm^{-1}. The peaks located at 144 (E_g), 199 (E_g) and 399 cm^{-1} (B_{1g}) are assigned to the Ti–O bending vibrations of TiO_2, and the peaks at 639 cm^{-1} (E_g) and 517 cm^{-1} (A_{1g} + B_{1g}) refer to Ti-O stretching vibrations [12, 13].

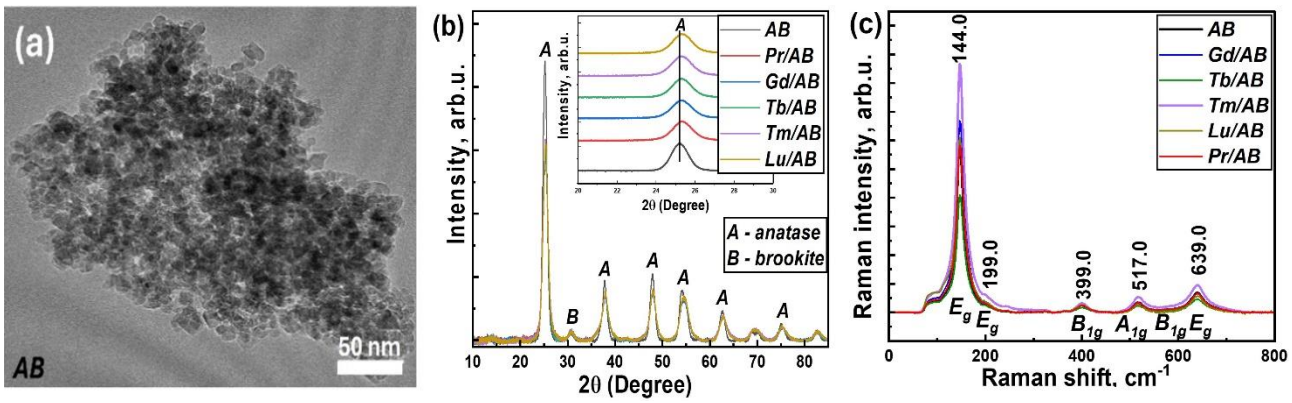

Figure 1 TEM-image (a), XRD patterns (b) and Raman spectra (c) of the samples

According to XRD studies, the phase content of brookite in unmodified *AB* was ~6%. Modification with Gd reduced the brookite content to ~4%, on the contrary modification with Pr increased it to ~9.4%. There were no peaks related to rare earth elements in the spectra of *RE/AB* (**Figure 1b**) due to their low concentration in the materials. The EDX spectra confirmed the presence of *RE* with the atomic ratio Ti:*RE* (Gd, Lu, Tm, Tb, Pr) ~1:0.013; 0.016; 0.016; 0.014; 0.012, respectively and Ti, O, C elements in *RE/AB* powders. The modified samples had an O/Ti ratio higher (2.52; 2.31; 2.72; 2.69; 2.96) than the stoichiometric value (2.0) because of water adsorption on the surface. The Ti-O and Ti-OH bonds in the samples were confirmed by FTIR analysis.

RE have larger ionic radii (0.0745–0.1045 nm) than Ti^{4+} (0.064 nm) therefore they can be distributed, create metal oxide clusters on the surface of TiO_2, occupy interstitial sites in the lattice of TiO_2 or form *RE*-O-Ti bonds [5, 6, 8, 9]. Such TiO_2 modification with *RE* can distort the crystal lattice, produce strain [14] and lead to crystallite size reduction. Indeed, the unit cell parameters and the unit cell volume were slightly decreased for *RE/AB* samples compared to *AB*. The broadening of the full width at half maximum (FWHM) and a slight shift

of all peaks towards higher 2θ were observed for modified samples in XRD patterns (**Figure 1b**) and can also indicate the appearance of the strain and crystallite size reduction. To obtain reliable information different methods were used for the calculation of these values (**Figure 2a, Table 1**).

All the methods confirmed the decrease of the crystallite size and increase of strain, stress, and energy density for *RE/AB* compared to *AB*. The samples *Pr/A-B* and *Tm/A-B* had the smallest crystallite size and the highest values of strain, stress, and energy density (**Figure 2a, Table 1**). Therefore, the modification of TiO_2 with rare earths induced stress in the lattice and inhibited the crystallites growth. Such decrease of the crystallite size resulted in an increase of the samples dislocation density meaning that TiO_2 modification with *RE* improved its strength and hardness [15].

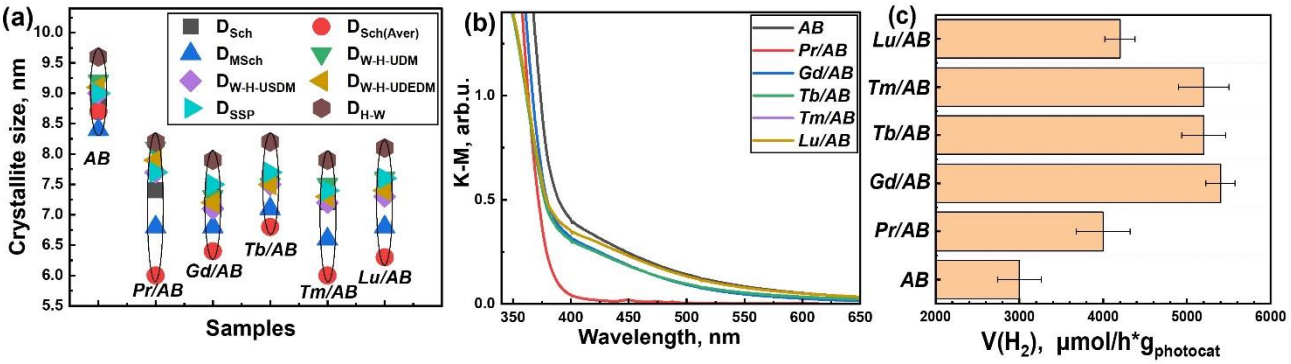

Figure 2 Crystallite size of the samples calculated by different methods(a), UV–Vis spectra (b) and photocatalytic hydrogen evolution from aqueous/ethanol solution in the presence of the obtained samples

Table 1 Strain (ε), stress (σ, MPa) and energy density (U, KJm^{-3}) of the samples calculated by different methods

Sample	W-H						SSP	H-W
	UDM	USDM		UDEDM				
	ε × 10^{-3}	ε × 10^{-3}	σ × 10^{-2}	ε × 10^{-3}	σ × 10^{-2}	U × 10^{-3}	ε × 10^{-2}	ε × 10^{-2}
AB	0.80	0.66	8.37	0.73	9.30	0.034	1.56	1.01
Pr/A-B	3.72	3.05	38.69	3.36	42.65	0.716	4.10	2.66
Gd/A-B	1.50	1.20	15.01	1.33	16.85	0.112	3.00	1.95
Tb/A-B	1.08	0.84	10.63	0.95	12.03	0.057	2.57	1.67
Tm/A-B	2.68	2.10	27.29	2.30	30.39	0.364	3.68	2.39
Lu/A-B	2.21	1.70	22.09	1.95	24.78	0.242	3.38	2.19

Table 2 Textural characteristics of the samples

Sample	*External surface area*, m^2/g	*Mesopore surface area*, m^2/g	*Specific surface area*, m^2/g	*Micropore volume*, cm^3/g	*Mesopore volume*, cm^3/g	*Total pore volume*, cm^3/g	*Pore diameter*, nm
AB	28	140	168	0.0074	0.211	0.273	6.6
Pr/AB	32	153	185	0.0051	0.248	0.309	6.5
Gd/AB	27	165	192	0.0046	0.246	0.298	6.2
Tb/AB	36	154	190	0.0041	0.233	0.302	6.4
Tm/AB	33	153	186	0.0033	0.220	0.286	6.1
Lu/AB	38	150	188	0.0038	0.220	0.299	6.3

Decreasing the crystallite size can also favour increasing the surface area of the samples. Indeed, the specific surface area for undoped *AB* was 168 m^2/g and higher for *RE/AB* (**Table 2**). The isotherms of the samples belong to type IV in accordance with IUPAC classification, namely type IVa with H2b type of hysteresis loop which is characteristic for mesoporous materials. In addition to mesopores the samples contained a negligible volume of micropores that decreased twice for *RE/AB* compared to *AB*.

Changes in the structural and textural characteristics of the *RE/AB* samples affected their optical band gap properties. The UV-Vis absorption spectra of the samples are shown in **Figure 2b**. The absorption edge of *RE/AB* samples was shifted to a shorter wavelength compared to *AB* that indicates an increase in the optical bandgap E_g of the composites. The bandgap for the direct and indirect transitions for *AB* were 3.33 and 3.11 eV, for *RE* (Gd, Lu, Tm, Tb, Pr)*/AB* – 3.37; 3.31; 3.34; 3.33; 3.41 eV and 3.13; 3.12; 3.13; 3.10; 3.16 eV, respectively. Such band gap widening of the nanomaterials is attributed to the dimensional limitation of photogenerated charge carriers in the nanoparticles. This phenomenon is known as quantum confinement or size quantization. The powders *Pr/AB* and *Tm/AB* had the smallest crystallites and the largest E_g.

The samples *RE/AB* demonstrated better photocatalytic performance in the photoreduction reaction of H_2 formation compared to *AB* (**Figure 2c**). The photocatalytic activity of *AB* modified with Gd, Tb and Tm is approximately twice as high than for unmodified and does not change for 5 consecutive cycles. The increase of photocatalytic activity of *RE/AB* samples seemed to be associated with the decrease of the crystallites size and increasing the specific surface area, i.e. the number of active reaction sites on the surface of photocatalysts increases. Rare earth elements can act as electron scavengers and consequently generate more electrons (e^-) available for the reaction, prevent their recombination and increase their lifetime [2]. Besides, brookite has a higher cathodic potential than anatase, which energetically favours the reduction of protons to produce H_2 [16]. Moreover, the presence of anatase–brookite heterojunctions has a positive effect on the activity of the samples mostly due to the increase of the number of charge carrier species available to participate in photoreactions at the photocatalyst surface [17].

4. CONCLUSION

In this work two-phase TiO_2 (anatase-brookite) modified with (Gd, Lu, Tm, Tb, Pr) was obtained by a one-step hydrothermal method. The influence of rare earth elements on morphology, crystal phase, optical, textural, and photocatalytic properties of *AB* was analysed. It was established that the modification inhibited the crystallite growth and induced stress in the TiO_2 lattice. The decreasing of crystallite size and increasing of strain, stress, and energy density values for *RE/AB* were confirmed by the Scherrer equation, modified Scherrer equation, the Williamson-Hall method based on a uniform deformation model, uniform stress deformation model, and uniform deformation energy density model approaches, size-strain plot (SSP) and the Halder-Wagner method. The IVa type of N_2 adsorption-desorption isotherms and H2b type of a hysteresis loop confirmed mesoporous structure of the prepared samples. Modification of TiO_2 with *RE* led to the increase of specific, external and mesopore surface area, total pore volume and mesopore volume. UV-Vis diffuse reflectance spectra of the modified samples showed a blue shift compared to *AB*. The band gap of the modified samples was increased due to a phenomenon of quantum confinement or size quantization. The modified samples showed higher photocatalytic activity in the reaction of photoreduction compared to *AB*.

ACKNOWLEDGEMENTS

This work was supported by the SARU-fellowship program for researchers at risk from Ukrainian universities and by the Technical University of Denmark.

REFERENCES

[1] EDDY, D.R., PERMANA, M.D., SAKTI, L.K., SHEHA, G.A.N., SOLIHUDIN, N., HIDAYAT, S., TAKEI, T., KUMADA, N., RAHAYU, I. Heterophase polymorph of TiO_2 (Anatase, rutile, brookite, TiO_2 (B)) for efficient photocatalyst: fabrication and activity. *Nanomaterials*, 2023, vol. 13, p. 704. https://doi.org/10.3390/nano13040704

[2] KHEDR, T.M., EL-SHEIKH, S.M., KOWALSKA, E., ABDELDAYEM, H.M. The synergistic effect of anatase and brookite for photocatalytic generation of hydrogen and diclofenac degradation. *Journal of Environmental Chemical Engineering*. 2021, vol. 9, p. 106566. https://doi.org/10.1016/j.jece.2021.106566

[3] NACHIT, W., AHSAINE, H.A., RAMZI, Z., TOUHTOUH, S., GONCHAROVA, I., BENKHOUJA, K. Photocatalytic activity of anatase-brookite TiO_2 nanoparticles synthesized by sol gel method at low temperature. *Optical Materials*. 2022, vol. 129, p. 112256. https://doi.org/10.1016/j.optmat.2022.112256

[4] SMIRNOVA, O.V., GREBENYUK, A.G., LOBANOV, V.V., KHALYAVKA T.A., SHCHERBAN N.D., PERMYAKOV V.V., SCHERBAKOV S.N. Experimental and quantum-chemical studies of electronic and spectral properties of titanium dioxide, modified with tin and lanthanum. *Applied Nanoscience*. 2023, vol. 13, pp. 5345–5355. https://doi.org/10.1007/s13204-023-02797-3

[5] KUTUZOVA, A., MORITZ, J.-O., MOUSTAKAS, N.G., DONTSOVA, T., PEPPEL, T., STRUNK, J. Performance of Sm-doped TiO_2 in photocatalytic antibiotic degradation and photocatalytic CO_2 reduction. *Applied Nanoscience*. 2023, vol. 13, pp. 6951–6966. https://doi.org/10.1007/s13204-023-02832-3

[6] MANDARI, K.K., POLICE, A.K.R., YEON, J., DO, KANG, M., BYON, C. Rare earth metal Gd influenced defect sites in N doped TiO_2: Defect mediated improved charge transfer for enhanced photocatalytic hydrogen production. *International Journal of Hydrogen Energy*. 2018, vol. 43, pp. 2073-2082. https://doi.org/10.1016/j.ijhydene.2017.12.050

[7] KHALYAVKA, T.A., SHCHERBAN, N.D., SHYMANOVSKA, V.V., MANUILOV E.V., PERMYAKOV V.V., SHCHERBAKOV S.N. Cerium-doped mesoporous $BaTiO_3/TiO_2$ nanocomposites: structural, optical and photocatalytic properties. *Res Chem Intermed*. 2019, vol. 45, pp. 4029–4042. https://doi.org/10.1007/s11164-019-03888-z

[8] MIKOLAJCZYK, A., WYRZYKOWSKA, E., MAZIERSKI, P., GRZYB, T., WEI, Z., KOWALSKA, E., CAICEDO, P.N.A., ZALESKA-MEDYNSKA, A., PUZYN, T., NADOLNA, J. Visible-light photocatalytic activity of rare-earth-metal-doped TiO_2: Experimental analysis and machine learning for virtual design. *Applied Catalysis. B, Environmental*. 2024, vol. 346, p. 123744. https://doi.org/10.1016/j.apcatb.2024.123744

[9] LI, H., ZHENG, K., SHENG, Y., SONG, Y., ZHANG, H., HUANG, J., HUO, Q., ZOU, H. Facile synthesis and luminescence properties of TiO_2:Eu^{3+} nanobelts. *Optics & Laser Technology/Optics and Laser Technology*, 2013, vol. 49, pp. 33–37. https://doi.org/10.1016/j.optlastec.2012.12.007

[10] KHALYAVKA, T.A., SHYMANOVSKA, V.V., MANUILOV, E.V., SHCHERBAN, N.D., KHYZHUN, O.Y., KORZHAK, G.V., PERMYAKOV, V.V. The influence of La Doping on structural, optical, and photocatalytic properties of TiO_2 in dyes destruction and hydrogen evolution. In: *Fesenko, O., Yatsenko, L. (eds) Nanomaterials and Nanocomposites, Nanostructure Surfaces, and Their Applications. Springer Proceedings in Physics*, Springer, Cham. 2020, vol. 246, pp. 361–380. https://doi.org/10.1007/978-3-030-51905-6_27

[11] ELAHIFARD, M., SADRIAN, M.R., MIRZANEJAD, A., BEHJATMANESH-ARDAKANI, R., AHMADVAND, S. Dispersion of Defects in TiO_2 Semiconductor: Oxygen Vacancies in the Bulk and Surface of Rutile and Anatase. *Catalysts*, 2020, vol. 10, p. 397. https://doi.org/10.3390/catal10040397

[12] RADHA, E., KOMARAIAH, D., SAYANNA, R., SIVAKUMAR, J. Photoluminescence and photocatalytic activity of rare earth ions doped anatase TiO_2 thin films. *Journal of Luminescence*. 2022, vol. 244, p. 118727. https://doi.org/10.1016/j.jlumin.2022.118727

[13] KOMARAIAH, D., RADHA, E., JAMES J., KALARIKKAL, N., SIVAKUMAR, J., REDDY, M.V.R., SAYANNA, R. Effect of particle size and dopant concentration on the Raman and the photoluminescence spectra of TiO_2:Eu^{3+} nanophosphor thin films. *Journal of Luminescence*. 2019, vol. 211, pp. 320-333. https://doi.org/10.1016/j.jlumin.2019.03.050

[14] PAUL, S., CHETRI, P., CHOUDHURY, B., AHMED, G.A., CHOUDHURY, A. Enhanced visible light photocatalytic activity of Gadolinium doped nanocrystalline titania: An experimental and theoretical study. *Journal of Colloid and Interface Science*. 2015, vol. 439, pp. 54–61. https://doi.org/10.1016/j.jcis.2014.09.083

[15] THEIVASANTHI, T., ALAGAR, M. Titanium dioxide (TiO_2) Nanoparticles XRD Analyses: An Insight. *arXiv (Cornell University)*. 2013. https://doi.org/10.48550/arxiv.1307.1091

[16] MANZOLI, M., FREYRIA, F.S., BLANGETTI, N., BONELLI, B. Brookite, a sometimes under evaluated TiO_2 polymorph. *RSC Advances*. 2022, vol. 12, pp. 3322–3334. https://doi.org/10.1039/d1ra09057g

[17] ŽERJAV, G., ŽIŽEK, K., ZAVAŠNIK, J., PINTAR, A. Brookite vs. rutile vs. anatase: What`s behind their various photocatalytic activities? *Journal of Environmental Chemical Engineering*. 2022, vol. 10, p. 107722. https://doi.org/10.1016/j.jece.2022.107722